



## Q[8]/SC[6]A-based framework constructed *via* OSIQ for metal ion capture

Li-Fei Tian<sup>a</sup>, Ming Liu<sup>a</sup>, Li-Xia Chen<sup>a</sup>, Chao Huang<sup>a</sup>, Qian-Jiang Zhu<sup>a</sup>, Kai Chen<sup>b,\*</sup>, Jiang-Lin Zhao<sup>c,\*</sup>, Zhu Tao<sup>a,\*</sup>

<sup>a</sup> Key Laboratory of Macrocyclic and Supramolecular Chemistry of Guizhou Province, Guizhou University, Guiyang 550025, China

<sup>b</sup> Jiangsu Collaborative Innovation Center of Atmospheric Environment and Equipment Technology, Jiangsu Key Laboratory of Atmospheric Environment Monitoring and Pollution Control, School of Environmental Science and Engineering, Nanjing University of Information Science & Technology, Nanjing 210044, China

<sup>c</sup> Institute of Biomedical & Health Engineering, Shenzhen Institute of Advanced Technology, Chinese Academy of Sciences, Shenzhen, 518055 China

### ARTICLE INFO

#### Article history:

Received 5 June 2021

Revised 19 August 2021

Accepted 24 August 2021

Available online 30 August 2021

#### Keywords:

Cucurbit[8]uril

4-Sulfocalix[6]arene

Outer surface interaction of Q[n]s

Supramolecular framework

Metal ion capture

### ABSTRACT

Since the outer surface interaction of Q[n]s (OSIQ, including self-, anion- and aromatic-induced OSIQs) was proposed in 2014, it has become the most important research area in our group to construct various Q[n]-based supramolecular frameworks *via* the OSIQ strategy. Herein, we report a novel supramolecular framework constructed using cucurbit[8]uril (Q[8]) and 4-sulfocalix[6]arene (SC[6]A). This Q[8]/SC[6]A-based supramolecular framework is a product *via* the perfect combination of self-, anion- and aromatic-induced OSIQs. This framework has the characteristics of easy preparation and high stability with the most important feature being the sequence selective capture of specific metal cations, such as common alkali- and alkaline earth metal ions, and renewability. Thus, this framework may be used in seawater desalination, potassium ion enrichment, radioactive cesium ion pollution source treatment, Gruinard's treatment or water softening and other applications.

© 2021 Published by Elsevier B.V. on behalf of Chinese Chemical Society and Institute of Materia Medica, Chinese Academy of Medical Sciences.

In general, cucurbit[n]urils (Q[n]s) contain  $n$  glycolurils bridged by  $2n$  methylene units and have two opening portals and a single rigid cavity (Fig. 1a) [1–5]. Thus, the structural properties of Q[n]s define the two main branches of Q[n]-chemistry: 1) Q[n]-based host–guest chemistry, which is related to the inclusion of various guests in the cavity of Q[n]s [6–11] and 2) coordination chemistry, which is related to the interaction between Q[n]s and metal ions ( $M^{n+}$ s) [12–15].

In the study of coordination between Q[n]s and  $M^{n+}$ s, we found by chance that inorganic anions, in particular, polychlorinated anions, always surround the outer surface of Q[n]s, which can promote the coordination between Q[n]s and  $M^{n+}$ s to form various coordination polymers [14,15]. The reason was attributed to the outer surface of Q[n]s presenting a positive electrostatic potential which interacts with electronegative species (Figs. 1c–e), improving the electronegative atmosphere of the ports of Q[n]s and enhancing the coordination chance of Q[n]s with  $M^{n+}$ s [16,17]. Further studies found that this characteristic of Q[n]s can also be reflected

in the interaction between Q[n]s. The electrostatic potential negative ports of a Q[n] always tend to be close to the electrostatic potential positive outer surface of adjacent Q[n]s, and these dipole interactions may become the driving force (Fig. 1c). In addition, aromatic compounds also tended to be near the outer surface of Q[n]s, and the  $\pi \cdots \pi$  interaction and C–H $\cdots$  $\pi$  interactions may also be the driving force (Fig. 1e). These effects related to the outer surface of Q[n]s have been found to play important roles in the coordination, supramolecular self-assemblies, and frameworks of Q[n]s. Therefore, we define these effects as the outer surface interactions of Q[n]s (OSIQ), which can be divided into self-, anion- and aromatic-induced OSIQs according to the characteristics of these effects, which have been summarized in a recent review [17].

Calix[n]arene (C[n]A) are macrocyclic compounds formed by  $n$  methylene groups connected to  $n$  benzene rings. They are similar to Q[n]s and also have a hydrophobic cavity [18–20]. In particular, a large number of aromatic rings in the structure could make them easy to form Q[n]/SC[n]A hybrids with framework features. So far, however, the related reports are rare [21,22]. As early as 2008, Long and co-workers chose 4-sulfocalix[n]arenes (SC[n]As;  $n = 4$  and 6; Fig. 1b) and Q[6] as building blocks, and constructed two novel Q[n]/SC[n]A-based frameworks [21]. We recently demonstrated a supramolecular aggregation of Q[7] and SC[4]A, which

\* Corresponding authors.

E-mail addresses: [kaichen85@nuist.edu.cn](mailto:kaichen85@nuist.edu.cn) (K. Chen), [jl.zhao@siaat.ac.cn](mailto:jl.zhao@siaat.ac.cn) (J.-L. Zhao), [gzttao@263.net](mailto:gzttao@263.net) (Z. Tao).

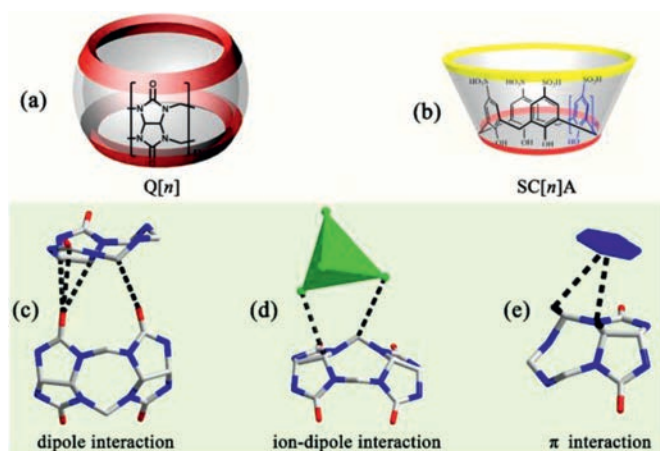


**Fig. 1.** (a, b) The molecular structures of Q[n]s and SC[n]As. (c–e) A schematic representation of the outer surface interactions formed between the Q[n] molecule and different compounds.

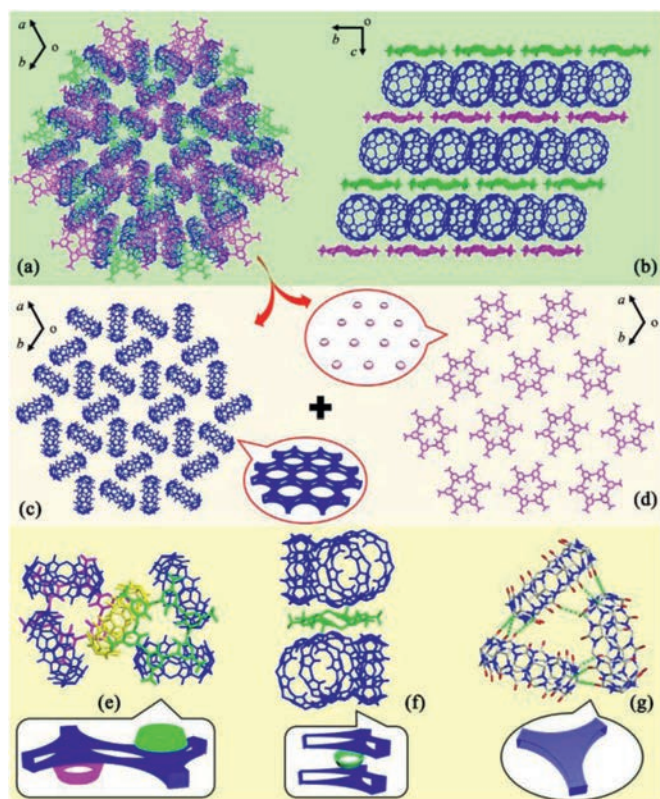


**Fig. 2.** Overview of the crystal structure of Q[8]/SC[6]A-based supramolecular framework **1** along the (a) *c*-axis and (b) *a*-axis. (c) Q[8]-based supramolecular layer and (d) SC[6]A-based layer. (e) Each Q[8] molecule accompanied by four Q[8] molecules and two SC[6]A via three types OSIQs. (f) Each SC[6]A molecule accompanied by six Q[8] molecules via the anion- and aromatic-induced OSIQs, and (g) a three-Q[8] unit.

can accommodate molecules of some volatile compounds or luminescent dyes [22].

In the present work, we selected Q[8] and 4-sulfocalix[6]arene (SC[6]A), which contain not only aromatic rings, but also anions, as building blocks and prepared a novel Q[8]/SC[6]A-based supramolecular framework in hydrochloric acid medium (**1**). Figs. 2a and b show an overview of the crystal structure of **1** along the *c*- and *a*-axis, respectively, which are formed by an alternating accumulation of Q[8]-layers (Fig. 2c) and SC[6]A-layers

(Fig. 2d). A close inspection reveals that each Q[8] molecule interacts with four adjacent Q[8] molecules in the framework via self-induced OSIQ (Figs. 1c and 2e) and interacts with two SC[6]A via anion- and aromatic-induced OSIQs (Figs. 1d, 1e and 2e). Two electrostatic potential negative portals of two of the four Q[8] molecules are close to the electrostatic potential positive outer surface of the central Q[8] molecule, whereas the two electrostatic potential negative portals of the central Q[8] molecule are close to the electrostatic potential positive outer surface of the another two Q[8] molecules. Basically, the interaction, between these adjacent Q[8] molecules is the dipole interaction, and the interaction distances are in the range of 2.996–3.404 Å (Figs. 1c and 2e). The anion- and aromatic-induced OSIQs can be observed even more clearly between the Q[8] molecule and SC[6]A molecule. Six Q[8] molecules are evenly distributed on both sides of a nearly flat chair structure SC[6]A molecule. The driving force include: 1) the anion-dipole interaction of  $\text{SO}_3^-$  anion in the SC[6]A molecule toward the electrostatic potential positive portal carbonyl carbon atoms, methine groups and methylene groups of the adjacent Q[8] molecules, respectively; 2) the  $\pi \cdots \pi$  interactions between the carbonyl groups of the adjacent Q[8] molecules and aromatic rings of the flat SC[6]A molecule; and 3) as well as the C–H $\cdots\pi$  interactions between the aromatic rings of the flat SC[6]A molecule and the methine and methylene groups on the outer surface of the adjacent Q[8] molecules (Fig. 2f). Moreover, two three Q[8] molecular combinations, which are distributed on both sides of molecule SC[6]A, form a triangular structure (three-Q[8] unit) via the self-induced OSIQ (Fig. 2g). Thus, framework **1** perfectly indicates the important role of the three types OSIQs in constructing Q[8]/SC[6]A-based supramolecular frameworks.

Further experiments showed that the preparation of **1** was very convenient. Simply mixing Q[8] and SC[6]A in aqueous neutral or weak acidic solutions can quantitatively obtain the desired supramolecular framework (**1**) as amorphous, microcrystalline, single crystals or even as a solution (see video in Supporting information). For example, titration  $^1\text{H}$  NMR experiments in  $\text{D}_2\text{O}$  show that the  $^1\text{H}$  NMR spectra of Q[8] seem to be sensitive to SC[6]A, even the presence of a tiny amount of SC[6]A. The proton resonance of Q[8] weakened rapidly, while the proton resonance of SC[6]A increased with the increase of SC[6]A concentration (Fig. S1 in Supporting information). This experimental phenomenon suggests that Q[8] and SC[6]A can easily form supramolecular framework (**1**), which is insoluble in aqueous solution.  $^1\text{H}$  NMR spectra of the framework in 6 mol/L HCl solution indicate that the molar ratio of SC[6]A/Q[8] is close to 1:3 (Fig. S2 in Supporting information). Titration  $^1\text{H}$  NMR experiments in  $\text{DCI}/\text{D}_2\text{O}$  (6 mol/L) show that the interaction products of Q[8] with SC[6]A can dissolve in acidic media because the proton resonances of both components can be observed over the whole titration process (Fig. S3 in Supporting information).

Dynamic light scattering (DLS) performed in an aqueous HCl solution was employed to monitor the formation of the Q[8]/SC[6]A-based supramolecular framework. Fig. S4 (Supporting information) shows the DLS data of the Q[8]/SC[6]A-based supramolecular framework in an aqueous HCl solution (3 mol/L). The experimental results showed that upon mixing Q[8] and SC[6]A at a molar ratio of 3:1 (0.2 mmol/L), the distribution of a hydrodynamic diameter centered at 2580 nm could be observed, indicating the formation of aggregates under the experimental conditions, providing circumstantial evidence for the supramolecular self-assembled solution structure between Q[8] and SC[6]A.

Isothermal titration calorimetry (ITC) measurements gave the physical and chemical data for the interaction between Q[8] and SC[6]A. The interaction molar ratio was 0.332, close to the 3:1 ratio of Q[8] to SC[6]A observed in the crystal structure analysis and the interaction association constant ( $K_a$ ) of Q[8] and SC[6]A was

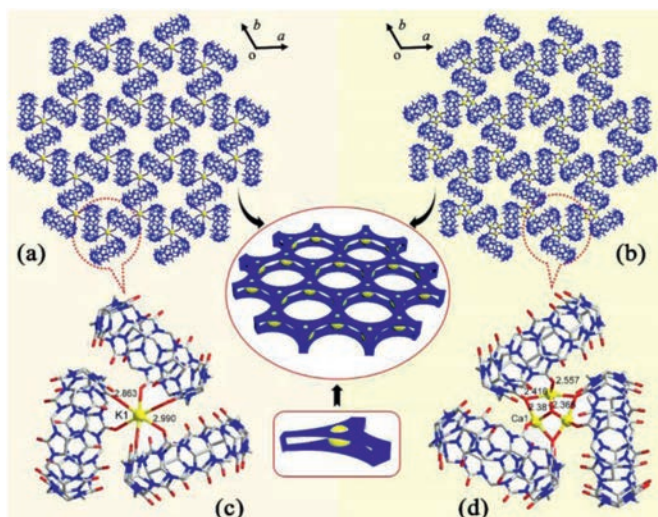


**Fig. 3.** Crystal structure of Q[8]-based 2D MOF with (a) K<sup>+</sup> and (b) Ca<sup>2+</sup> cations and the three-Q[8] unit with (c) K<sup>+</sup> and (d) Ca<sup>2+</sup> cation.

determined to be  $(3.71 \pm 0.61) \times 10^4$ . Moreover, both negative enthalpy and entropy indicates that the assembly process is only driven by favorable enthalpy change rather than entropy change (Fig. S5 in Supporting information).

A large number of microcrystals was appeared after evenly stirring of two components for a while and the X-ray powder diffraction results were consistent with the theoretical results obtained in an aqueous HCl solution (3 mol/L) (Fig. S6 in Supporting information). Generally, Q[*n*]s can coordinate with M<sup>*n*+</sup>s to form various complexes and coordination polymers due to the ion-dipole interaction of electrostatic potential negative portal carbonyl oxygen atoms with M<sup>*n*+</sup> cations and their coordination ability with M<sup>*n*+</sup>s depends on the distribution density of the portal carbonyl oxygen atoms. Therefore, smaller Q[*n*]s, such as Q[5] and Q[6], generally have a strong coordination ability with M<sup>*n*+</sup>s, and larger Q[*n*]s, such as Q[7], Q[8], Q[10] [14,15,23], are generally weaker in coordination with M<sup>*n*+</sup>s [14,15]. However, if we can increase the distribution density of portal carbonyl oxygen atom of the larger Q[*n*]s, such as the construction of Q[*n*]-based frameworks, the coordination ability of the larger Q[*n*]s with metal ions may be improved. In this way, we have synthesized a Q[10]-based framework, in which the triangle region formed by Q[10] molecules can selectively capture a variety of metal ions [23]. Looking at the Q[8]-based supramolecular framework in the Q[8] layer (Fig. 2c) of the Q[8]/SC[6]A-based supramolecular framework, we found that there are a large number of three-Q[8] units which show a high density of portal carbonyl-oxygen atoms, so it can be inferred that this area should be able to accommodate M<sup>*n*+</sup>s (Fig. 2g). Thus, we carried out a study on the interaction of the Q[8]-SC[6]A system with various M<sup>*n*+</sup>s and the results showed that the Q[8]/SC[6]A-based supramolecular framework shows selectivity toward M<sup>*n*+</sup>s with larger ionic radii, such as alkali metal ions (A<sup>+</sup>), alkaline earth metal ions (AE<sup>2+</sup>), and even lanthanide cations (Ln<sup>3+</sup> will be discussed specifically). Crystal structure analysis revealed that the Q[8]/SC[6]A-A<sup>+</sup> systems can yield similar frameworks to that of **1**, but the Q[8]-based 2D supramolecular frameworks are filled with the selected metal ions *via* direct coordination to form Q[8]/A<sup>+</sup>-based 2D metal-organic frameworks, in which each three-Q[8] unit captures a metal ion. Fig. 3a and Fig. S7 (Supporting information) show the Q[8]-based 2D framework in the Q[8]/SC[6]A/A<sup>+</sup> supramolecular framework for K<sup>+</sup> ion capture as a representative, in which each three-Q[8] triangle unit accommodates a K<sup>+</sup> cation *via* direct coordination. The interaction dis-

tances (O<sub>carbonyl</sub>-A<sup>+</sup>) are in the range of 2.863–2.990 Å (Fig. 3c). Another three similar Q[8]/SC[6]A/A<sup>+</sup> supramolecular frameworks (A<sup>+</sup> = Na<sup>+</sup>, Rb<sup>+</sup> and Cs<sup>+</sup>, respectively) were also obtained. Fig. S8 (Supporting information) shows the differences in the interaction distances (O<sub>carbonyl</sub>-A<sup>+</sup>) in the three-Q[8]-A<sup>+</sup> units among these frameworks and the related crystal data are shown in Table S1 (Supporting information). It is interesting that when comparing the ionic radii of the A<sup>+</sup> cation and their variation (0.97, 1.33, 1.47, 1.67 Å for Na<sup>+</sup>, K<sup>+</sup>, Rb<sup>+</sup> and Cs<sup>+</sup>, respectively with the maximum change being ~0.7 Å), the average interaction distances are 2.886, 2.926, 2.988 and 3.062 Å for Na<sup>+</sup>, K<sup>+</sup>, Rb<sup>+</sup> and Cs<sup>+</sup> with the maximum change being only ~0.2 Å. This suggests that the 2D Q[8]-based supramolecular framework is quite rigid due to the comprehensive OSIQs derived from the Q[8] and SC[6]A components. For the Q[8]-SC[6]A-AE<sup>2+</sup> systems, the crystal structures of the Q[8]/SC[6]A/Ca<sup>2+</sup>- and Sr<sup>2+</sup>-based frameworks were obtained. Although many attempts have been made, the Q[8]-SC[6]A-Ba<sup>2+</sup> system immediately produce a precipitate. Similar to the Q[8]/SC[6]A/K<sup>+</sup>-based framework, the Q[8]/SC[6]A/Ca<sup>2+</sup>- and Sr<sup>2+</sup>-based frameworks also have similar structural features with alternative Q[8]-layers and SC[6]A-layers, but in the 2D Q[8]-based MOF (Fig. 3b), the three-Q[8] unit can accommodate a Ca<sup>2+</sup> or Sr<sup>2+</sup> cation with 1/3 occupancy at three positions. The interaction distances were in the range of 2.381–2.557 Å for the Ca-case as a representative (Fig. 3d), and the related crystal data shown in Table S1. Although we failed to obtain the single crystal structure, the powder diffraction spectrum is given in Fig. S9 (Supporting information). For the Q[8]-SC[6]A systems with other metal ions, such as transition metal ions with smaller ionic radii, they always generated Q[8]/SC[6]A supramolecular frameworks identical to **1** and the related crystal data are shown in Table S2 (Supporting information).

The corresponding energy-dispersive spectra (EDS) of these solid crystals further confirmed these results. Figs. S10–S13 (Supporting information) show that EDS of the products from the Q[8]-SC[6]A-A<sup>+</sup> systems contain their corresponding metals Na, K, Rb and Cs, respectively. Figs. S15–S17 (Supporting information) show that the EDS of the products from the Q[8]-SC[6]A-AE<sup>2+</sup> systems contain their corresponding metals Ca, Sr and Ba, respectively. The ionic radii of these metal ions are generally close to or larger than 1 Å. For the Q[8]-SC[6]A-M<sup>*n*+</sup> systems in which the ionic radii of their related metal ions are smaller, the EDS of the products from these systems show no related metals, including Mg, Co, Mn, Ni, Fe, Cr, Al and Cu (Figs. S14, S18–S24 Supporting information). The anion- and aromatic-induced OSIQs between the Q[8] and SC[6]A molecules, and the self-induced OSIQ between the Q[8] molecules in framework **1** determine the rigid feature of the 2D Q[8]-based framework and size of the three-Q[8] molecule unit, thus determining the size of metal ions that the Q[8]-based layer can accommodate.

Considering the specific structural size of the three-Q[8] unit in the 2D Q[8]-based framework, it may be selective toward metal ions with different sizes, charges and other characteristics. For this reason, we specifically investigated the selectivity of **1** toward different metal ions, which can be captured in detail. Indeed, the EDS experimental results (Figs. S25–S34 in Supporting information) show that for the alkali metal series, **1** first traps K<sup>+</sup>, then Na<sup>+</sup>, then Cs<sup>+</sup>, and finally Rb<sup>+</sup> ions; for the alkaline earth metal series, **1** first traps Ba<sup>2+</sup>, followed by Sr<sup>2+</sup> and Ca<sup>2+</sup> ions (Figs. S35–S38 in Supporting information); for A<sup>+</sup> and AE<sup>2+</sup> ions, **1** prefers to capture AE<sup>2+</sup> ions (Figs. S39–S41 in Supporting information). The selective order of the metal ions that can enter the 2D Q[8]-based framework in **1** was Ba<sup>2+</sup> > Sr<sup>2+</sup> ≈ Ca<sup>2+</sup> > K<sup>+</sup> > Na<sup>+</sup> > Cs<sup>+</sup> > Rb<sup>+</sup>. Obviously, the selectivity toward metal ion trapping in framework **1** was related to not only the size of the ions, but also the valence state. The higher the valence state of the ions under the

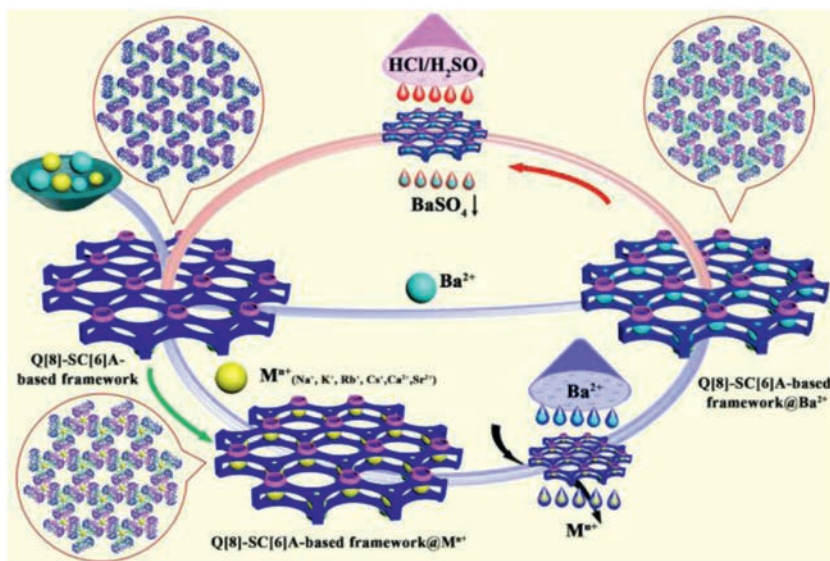


Fig. 4. Representative cycle of **1** for the capture of M<sup>n+</sup> ions.

premise of ensuring the size of the ions, the stronger the action of the ions with the portal carbonyl oxygen atoms in Q[*n*]s.

In our previous work, we used recyclable Q[*n*]-based frameworks to selectively capture metals. For example, Q[10]-based frameworks in aqueous HCl media were used to selectively trap different metal ions, the trapped metal ions were released in aqueous HNO<sub>3</sub> media and Q[10] can be recovered as a different Q[10]-based framework [23]. Similarly, the Q[8]-based frameworks in aqueous HCl media were used to selectively trap [AuCl<sub>4</sub>]<sup>-</sup> anions, which were reduced to gold in aqueous N<sub>2</sub>H<sub>4</sub>·H<sub>2</sub>O solution and Q[8] was recovered for reuse [24]. Naturally we would like to try to release the captured metal ions in different media and recycle **1** for reuse. However, attempts in various media, such as neutral water, various inorganic acids including HNO<sub>3</sub>, H<sub>2</sub>SO<sub>4</sub>, HClO<sub>4</sub> and H<sub>3</sub>PO<sub>4</sub>, organic acids including CHO<sub>2</sub>H, CH<sub>3</sub>CO<sub>2</sub>H and CF<sub>3</sub>CO<sub>2</sub>H, and alkaline media (NH<sub>3</sub>·H<sub>2</sub>O) all failed, but the Q[8]/SC[6]A/A<sup>+</sup> or AE<sup>2+</sup>-based frameworks exhibited exceptional stability. The experimental results show the products still hold the captured metal ions. How can we release the metal ions from the Q[8]/SC[6]A/M<sup>n+</sup>-based frameworks and recycle **1** for reuse? Although the Q[8]/SC[6]A/M<sup>n+</sup>-based frameworks are stable and cannot be disassembled to release the captured metal ions, the selectivity of **1** towards metal ions could be utilized to obtain a Q[8]/SC[6]A/M<sup>n+</sup>-based framework, from which the M<sup>n+</sup> can be easily removed so that **1** can be recovered and reused. For example, Ba<sup>2+</sup> ions can substitute other M<sup>n+</sup> ions from another Q[8]/SC[6]A/M<sup>n+</sup>-based framework to produce the most stable insoluble Ba<sup>2+</sup>-based self-assembly. Replacement experiments confirm that Ba<sup>2+</sup> ions can indeed replace other ions that have been captured in framework **1** (Figs. S42–S45 in Supporting information). It is well known that BaSO<sub>4</sub> is one of the most difficult substances to dissolve and whether the captured Ba<sup>2+</sup> ions can be forced to precipitate out of the self-assembly becomes key to regenerating **1**. H<sub>2</sub>SO<sub>4</sub>/HCl mixed acid solutions can be used to remove Ba<sup>2+</sup> ions and recover framework **1**. H<sub>2</sub>SO<sub>4</sub> was used to trap Ba<sup>2+</sup> ions in the insoluble Ba<sup>2+</sup>-based self-assembly to transform insoluble BaSO<sub>4</sub>, while concentrated HCl solutions, for example, aqueous 6 mol/L HCl solution, can be used to dissolve framework **1**. Therefore, the amount of H<sub>2</sub>SO<sub>4</sub> is generally required to be as small as possible, so that Ba<sup>2+</sup> in the Q[8]/SC[6]A/Ba<sup>2+</sup>-based self-assembly can be completely precipitated, while a sufficient amount of aqueous HCl solution is required so that the Q[8]/SC[6]A-based framework can

be fully dissolved. Our design (Fig. 4) was confirmed by the experimental results obtained under the optimal conditions in which 8 mL of the mixed acid (0.024 mol/L H<sub>2</sub>SO<sub>4</sub>/6 mol/L HCl) was used to treat 0.18 g of the Q[8]/SC[6]A/Ba<sup>2+</sup>-based self-assembly (Fig. S46 in Supporting information).

In summary, Q[8] and SC[6] were selected as building blocks, and a supramolecular framework (**1**) was synthesized. Structural analysis showed that **1** is formed by alternating Q[8]-layers and SC[6]A-layers via the perfect combination of OSIQs, including self-, anion- and aromatic-induced OSIQs. A study of its properties revealed that this framework was not only easy to construct, but also stable. Moreover, **1** exhibits the sequential selective capture of alkali- and alkaline earth metal ions due to the existence of 2D Q[8]-based framework layers with numerous three-Q[8] units. The selectivity order is Ba<sup>2+</sup> > Sr<sup>2+</sup> ≈ Ca<sup>2+</sup> > K<sup>+</sup> > Na<sup>+</sup> > Cs<sup>+</sup> > Rb<sup>+</sup>. The sequence selectivity of **1** towards metal ions can be utilized to obtain the most stable insoluble Ba<sup>2+</sup>-based self-assembly to release other captured metal ions, whereas H<sub>2</sub>SO<sub>4</sub>/HCl mixed acids can precipitate the captured Ba<sup>2+</sup> ions to release framework **1** which can be recovered and reused. Thus, the framework **1** may be used in seawater desalination, potassium ion enrichment, radioactive cesium ion pollution source treatment, guinard's treatment or water softening and other applications [25–28].

#### Declaration of competing interest

The authors declare no conflict of interest.

#### Acknowledgments

We thank the National Natural Science Foundation of China (Nos. 21871064, 21601090, 21761007, 51663005), Science and Technology Plan Project of Guizhou Province (Nos. 20175788 and 20185781). Dr. Jiang-Lin Zhao thanks the Basic Research Program of Shenzhen (No. JCYJ20190812151405298) and Shenzhen Peacock Plan.

#### Supplementary materials

Supplementary material associated with this article can be found, in the online version, at doi:10.1016/j.ccl.2021.08.106.

**References**

- [1] W.A. Freeman, W.L. Mock, N.Y. Shih, *J. Am. Chem. Soc.* 103 (1981) 7367–7368.
- [2] A.I. Day, A.P. Arnold, R.J. Blanch, (Unisearch Limited, Australia), PCT Int. Appl. 2000, WO2000-2000AU412 20000505, 112 (Priority: AU 99-232 19990507), 2016.
- [3] J. Kim, I.S. Jung, S.Y. Kim, et al., *J. Am. Chem. Soc.* 122 (2000) 540–541.
- [4] A.I. Day, R.J. Blanch, A.P. Arnold, et al., *Angew. Chem. Int. Ed.* 41 (2002) 275–277.
- [5] X.J. Cheng, L.L. Liang, K. Chen, et al., *Angew. Chem. Int. Ed.* 52 (2013) 7252–7255.
- [6] K. Kim, N. Selvapalam, Y.H. Ko, et al., *Chem. Soc. Rev.* 36 (2007) 267–279.
- [7] K.I. Assaf, W.M. Nau, *Chem. Soc. Rev.* 44 (2015) 394–418.
- [8] W. Liu, S.K. Samanta, B.D. Smith, L. Isaacs, *Chem. Soc. Rev.* 46 (2017) 2391–2403.
- [9] J. Murray, K. Kim, T. Ogoshi, W. Yao, B.C. Gibb, *Chem. Soc. Rev.* 46 (2017) 2479–2496.
- [10] R. Pinalli, A. Pedrini, E. Dalcanale, *Chem. Soc. Rev.* 47 (2018) 7006–7026.
- [11] J. Mosquera, Y. Zhao, H. Jang, et al., *Adv. Funct. Mater.* (2019) 190208.
- [12] O.A. Gerasko, M.N. Sokolov, V.P. Fedin, *Pure Appl. Chem.* 76 (2004) 1633–1646.
- [13] J. Lü, J.X. Lin, M.N. Cao, R. Cao, *Coord. Chem. Rev.* 257 (2013) 1334–1356.
- [14] X.L. Ni, X. Xiao, H. Cong, et al., *Chem. Soc. Rev.* 42 (2013) 9480–9508.
- [15] X.L. Ni, S.F. Xue, Z. Tao, et al., *Coord. Chem. Rev.* 287 (2015) 89–113.
- [16] X.L. Ni, X. Xiao, H. Cong, et al., *Acc. Chem. Res.* 47 (2014) 1386–1395.
- [17] Y. Huang, R.H. Gao, X.L. Ni, et al., *Angew. Chem. Int. Ed.* 60 (2021) 15166–15191.
- [18] X.Y. Lou, Y.P. Li, Y.W. Yang, *Biotechnol. J.* 14 (2019) 1800354.
- [19] H. Zhang, R. Zou, Y. Zhao, *Coord. Chem. Rev.* 292 (2015) 74–90.
- [20] O. Bistri, O. Reinaud, *Org. Biomol. Chem.* 13 (2015) 2849–2865.
- [21] R.G. Lin, L.S. Long, R.B. Huang, L.S. Zheng, *Cryst. Growth Des.* 8 (2008) 791–794.
- [22] X. Tian, L.X. Chen, Y.Q. Yao, et al., *ACS Omega* 3 (2018) 6665–6672.
- [23] Y.Q. Yao, Y.J. Zhang, C. Huang, et al., *Chem. Mater.* 39 (2017) 5468–5472.
- [24] L.X. Chen, M. Liu, Y.Q. Zhang, et al., *Chem. Commun.* 55 (2019) 14271–14274.
- [25] Z. Zeng, Y. Zhang, X. Zhang, et al., *Chin. Chem. Lett.* 32 (2021) 2572–2576.
- [26] X. Qian, S. Deng, X. Chen, et al., *Chin. Chem. Lett.* 31 (2020) 2211–2214.
- [27] N. Liu, L. Shia, X. Han, et al., *Chin. Chem. Lett.* 31 (2020) 386–390.
- [28] X. Li, T. Lu, Y. Wang, Y. Yang, *Chin. Chem. Lett.* 30 (2019) 2318–2322.